ORIGINAL PAPER

Positron Microscopy Studies of Wear Tracks on a Copper Surface

Jerzy Dryzek · Shigehiro Nojiri · Masanori Fujinami

Abstract Positron microscopy was used for studies of defects induced by ball indentation or sliding on the surface of well-annealed copper samples. A focused positron beam of 24.5-keV energy was used to scan the deformed region of the indenter impression, and measurements of the annihilation line parameter were performed. In the case of ball indentation, the measured defect distribution correlates well with the von Mises stress distribution of the Hertz contact and the von Mises yield criterion. For the wear track produced by pin on disc dry sliding, an asymmetric defect distribution near the wear track is observed. It indicates the presence of a tangential force that additionally deforms the sample.

Keywords Positron annihilation · Positron microscopy · Wear track · Indentation

1 Introduction

Deformation of ductile metals and alloys can be considered within two approaches, i.e., macroscopic or microscopic. The common macroscopic approach used by engineers is

J. Dryzek (✉)
Institute of Nuclear Physics PAN, ul. Radzikowskiego 152, 31-342 Kraków, Poland
e-mail: jerzy.dryzek@ifj.edu.pl

J. Dryzek
Institute of Physics, Opole University, ul. Oleska 48, 45-052 Opole, Poland

S. Nojiri · M. Fujinami
Department of Applied Chemistry, Chiba University, 1-33 Yayoi, Inage, Chiba 263-8522, Japan

based on the elastic theory, which links the material constants, i.e., Young's modulus, yield stress, etc., with the stress and/or residual stress. The microscopic approach is common for solid-state physicists or metallurgists. They consider the processes at the crystal lattice or atomic level. In this case, the deformation changes the shape of grains and creates new grain boundaries and an internal structure inside grains. In more detail, this is due to the slip of dislocations, which can dissociate to form stacking faults and/ or twinning in some conditions. Generally, dislocations are accompanied by the halo of vacancies and interstitial atoms easily created during their slip and crossing.

Experimental investigations of these processes successfully employ mainly TEM or SEM; nevertheless, other techniques, such as electrical resistivity measurements and XRD, are also applied. The positron annihilation technique is applied as well; however, it is not commonly used for this purpose. We recommend this technique because of its high sensitivity and selectivity to the open volume crystalline defects.

This technique is based on the fact that a positron implanted into a sample can be trapped at open volume defects such as vacancies, their clusters or jogs at dislocation lines [1]. Its annihilation with an electron results in emission in two opposite directions of two photons, which take over the energy and momentum of the annihilated pair. The momentum tags a local electron density, which is significantly lower in open volume defects than in a perfect host. This is reflected in the shape of the annihilation line and positron lifetime. Measurements of the broadening of the annihilation line or positron lifetime in the sample allow us to obtain useful information about defects induced for instance by plastic deformation. The positron annihilation techniques are very sensitive, and their selectivity to open volume defects is extremely high. This is because a positron

is positively charged, and before trapping, it scans a relatively large volume at the atomic scale. The positron techniques are non-destructive and allow us to study samples without special preparation, which could change their initial state. It is also possible to link residual stress or strain in the deformed sample and the positron characteristics, such as the so-called S-parameter (defined below) or mean positron lifetime. However, due to the high sensitivity, only a limited range of stress or strain values can be detected. For large stress and consequently large defect accumulation, saturation of the positron characteristics takes place [2, 3].

The development of the positron beam technique [4] resulted in the construction of the so-called positron microscopy [5]. In this case, moderated positrons are accelerated to a desired energy and formed in a beam. Using a special technique for beam focusing, one can obtain a beam width, i.e., a spot on the surface of the sample of about a dozen micrometers. In such a case, by scanning the surface of a deformed sample with a focused beam, one can obtain a 1D or 2D map of the measured positron characteristics. Today this technique allows us to obtain maps of either the mean positron lifetime or the S-parameter. This provides possibilities to conduct new research at the atomic level on plastically deformed samples.

The well-annealed copper samples were the object of our studies. It was found that in copper samples exposed to dry sliding, the zone with open volume defects is constituted below the worn surface. The zone thickness is quite large as it extends up to hundreds of micrometers depending on the applied load and sliding velocity. The characteristic feature of this zone is that the defect concentration decreases exponentially with the depth increase from the worn surface [7]. It was found that the large clusters, which consist of about ten vacancies, are created in the zone [8]. The clusters can be formed as a result of dislocation motions, which are created during plastic deformation. The electron microscope studies of plastically deformed copper single crystals have shown that after a small amount of deformation (close to 20 %), dislocation layers parallel to the slip planes occur. When deformation increases, the dislocation density increases [9]. The dislocations in motion can create interstitial atoms as well as vacancies, which can coalescence and be detected by positrons. We believe that copper is a suitable object for positron microscope studies because of the great sensitivity of positrons to vacancy clusters.

In this article, we report the use of the positron microscopy for the investigation of wear tracks, which are created when the pin in the tribo-tester slides on the surface of a copper sample. This is a common test performed for tribological studies. Up to now, our interest has been focused on regions extending into the interior, i.e., below

the surface of samples damaged during sliding. Positron microscopy gives us a unique opportunity to detect the distribution of defects directly on the surface. For comparison, static ball indentation studies are also performed. The positron annihilation results are compared with theoretical calculations based on the Hertz relations.

2 The Experimental Details

2.1 Sample Preparation

Samples of pure copper (purity of 99.99 %) in the form of discs, 2 cm in diameter and 2 mm thick, were annealed for 1 h at the temperature of 550 °C in the stream of N_2. This allows us to obtain virgin samples with only residual defects. The measurements of the positron lifetime for these samples revealed only single lifetime components equal to 120 ± 1 ps. The surfaces of these samples were exposed to static indentation with a 4-mm-diameter martensite steel ball with different loads similarly to the Rockwell hardness test. Other samples were put into the pin-on-disc tester, and a 4-mm-diameter steel ball was slid on its surface at a speed of 5 cm/s with a normal load of 25 N. The wear track diameter was 16 mm. Different numbers of cycles were performed: a single cycle, five and ten cycles or runs. The surfaces of these samples were investigated using the positron microscope constructed at Chiba University in Japan [5, 6].

2.2 Positron Measurements

The positron measurement was performed using a 24.5-keV positron beam of energy with a ca. 70-μm-diameter spot scanning the surface of the copper sample perpendicularly. The average depth below the surface at which positrons were implanted was about 0.6 μm. Thus, from the engineering point of view, only the surface regions are scanned by the positron beam. The sample was moved with a table in such a way that different regions of the damaged sample were illuminated by the beam. The HpGe detector was used for monitoring the annihilation line that occurs when positrons are annihilated in the sample. The positron microscope was described in detail by Fujinami et al. [5] and Oshima et al. [6]. The line shape parameter, called the S-parameter, is the main interest. This parameter is defined as the integral of the central part of the annihilation line normalized to the total integral of the line centered at 511 keV. It has been well proven experimentally that this parameter is extremely sensitive to the presence of open volume defects, such as a vacancy or its clusters and jogs at dislocation lines, where positrons are trapped. Thus, the change in the S-parameter value results

from a change of in the vacancy or vacancy cluster concentration and/or their size. For the virgin sample where only residual defects are present, the S-parameter has the lowest value. This indicates the bulk value. The link between the S-parameter value and the defect concentration can be well understood within the commonly used two-state trapping model (see Ref. [10]). The large defect concentration causes all positrons to be trapped, and the S-parameter value is saturated. This can also be easy to demonstrate for samples exposed to compression. In Fig. 1, we depicted the experimental dependency of the S-parameter on the thickness reduction of the compressed copper samples. A linear increase of the S-parameter value with an increase of the thickness reduction up to 10 % is
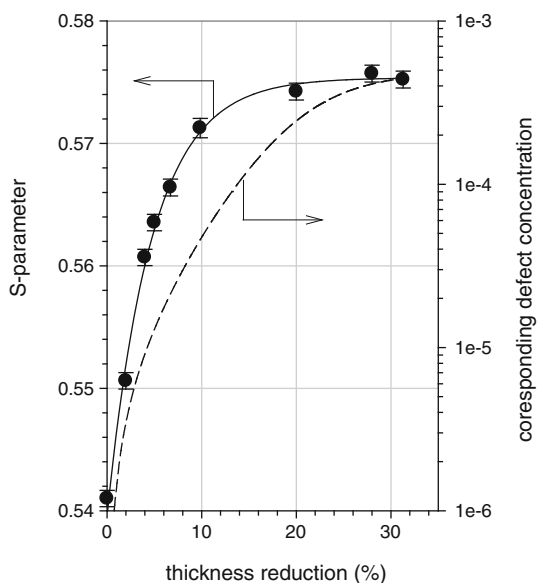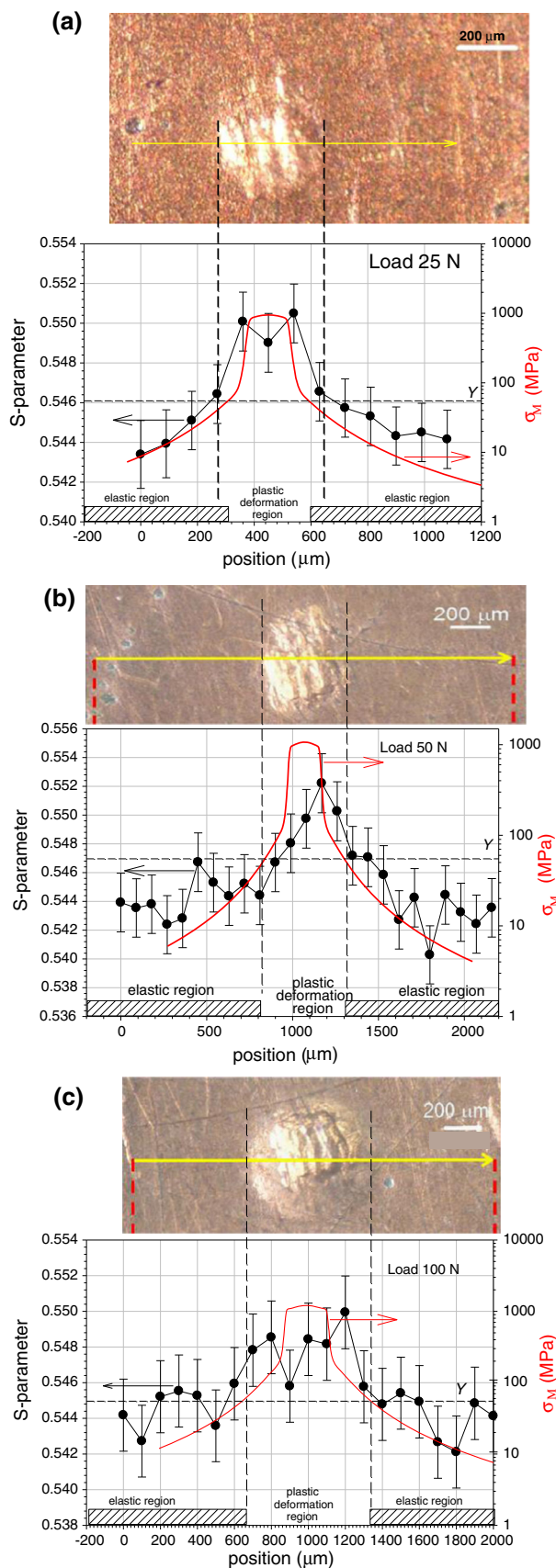

Fig. 1 The dependency of the measured S-parameter on the thickness reduction of the virgin copper samples exposed to compression. The *solid line* represents the best fit of the following equation: $S = S_{sat} + (S_{bulk} - S_{sat}) \exp(-c\varepsilon)$, where $S_{sat} = 0.5754 \pm 0.0005$, $S_{bulk} = 0.5395 \pm 0.0007$, $c = 0.212 \pm 0.010$, and ε is the thickness reduction expressed in %. The *dashed line* represents the dependency, which, according to the trapping model, links the vacancy concentration and S-parameter as follows: $C_v = (S - S_{bulk})/[(S_{sat} - S)\tau_{bulk}\mu_v]$, where μ_v is the specific trapping rate, and $\tau_{bulk} = 118$ ps for pure copper. The specific trapping rate is assumed equal to 1.1×10^{15} s^{-1} [18]

clearly visible. However, its further increase is nonlinear, and above 20 % the S-parameter value is saturated. This kind of dependency can be observed for other metals exposed to deep deformation and can be used as a link between the measured S-parameter and the strain of a deformed sample. The dashed line in this figure represents the approximate dependency of the vacancy concentration (see Fig. 1).

3 Experimental Results

3.1 Results for the Ball Indentation with Different Loads

The plastically deformed region induced by ball indentation was first investigated. The top of Fig. 2a presents the SEM picture of the indenter impression induced by the ball normally loaded with 25 N. Its diameter is about 290 μm. A horizontal arrow in the picture indicates the direction of the positron beam scan. In the lower part of Fig. 2a, the measured dependence of the S-parameter for different positions of the beam (left axis) is depicted. The increase in its value in the indentation region is clearly visible, which indicates the large accumulation of open volume defects. The vertical dashed lines indicate the impression indentation estimated from the top picture. It is also clearly visible that the S-parameter decreases slowly to the bulk value (about 0.5440 ± 0.0016) outside the dashed lines up to about 200 μm on both sides of the impression. Therefore, the damaged region induced by the indentation is slightly extended beyond the impression visible in the SEM picture.

Dryzek [11] reported the correlation between the S-parameter dependencies and so-called expanding cavity model proposed by Johnson [12] (see also [13]), which describes the plastic deformation beneath the ball indenter. In this model, the plastic deformation in the vicinity of the indenter is compared to that which occurs during the radial expansion of a spherical cavity subjected to internal pressure. Johnson replaced the expanding spherical cavity with an incompressible, hemispherical core of material directly beneath the indenter of the radius equal to the contact circle, a, Eq. (1). The core hemisphere is surrounded by a hemispherical plastic zone, which connects with the elastically strained material at some radius. The radius of the contact circle and core hemisphere can be calculated using the Hertz radius [14]:

$$a = \sqrt[3]{\frac{4}{3} \frac{k P R}{E}}, \tag{1}$$

where P is the normal load, R is the radius of the ball, and k is the elastic mismatch parameter given by

Table 1 The value of the contact radius calculated from Eq. (1) for different normal loads applied to the indenter and the measured indentation diameter on the surface of the annealed copper sample

Load (N)	a (μm)	Indentation diameter (μm)
25	70.5	290
50	88.9	490
100	112.0	670

$k = 9[(1 - v^2) + E(1 - v'^2)/E']/16$. Here, E, E' and v, v' are the Young's modulus, Poisson's ratio of the sample and indenter material, respectively. The radius of the plastic hemisphere can be estimated from the von Mises criterion for yield as follows, i.e., $\sigma_M = Y$, where Y is the yield strength for soft copper equal to 55 MPa and $\sigma_M = \sqrt{\frac{1}{2} \left[(\sigma_1 - \sigma_2)^2 + (\sigma_2 - \sigma_3)^2 + (\sigma_3 - \sigma_1)^2 \right]}$ is the von Mises stress, where σ_{1-3} are principal stresses; see "Appendix". Using relation (2)–(9), it is easy to calculate the σ_M at the surface, $z = 0$, and the solid line represents the obtained dependency; the right axis is in logarithmic scale. The value of the Hertz radius, a, for a load of 25 N is equal to 70.5 μm; however, the diameter of the impression is about 290 μm; see Table 1. The von Mises criterion allows us to separate the plastically and elastically deformed regions. In Fig. 2a, the hatched region corresponds to the elastically deformed region. It shows that the theoretical calculations correspond well with the impression indentation visible in the SEM picture; however, the S-parameter dependency extends beyond this region. This indicates the presence of open volume defects created during the elastic deformation, i.e., $\sigma_M < Y$. The high sensitivity of positrons allows us to detect them in this region, too.

Generally, the observation for the normal load of 25 N (Fig. 2a) is also valid for other applied loads. The increase of the normal load causes an increase of the Hertz radius and the indentation diameter; see Table 1 and Fig. 2b, c. For the load of 50 N (Fig. 2b), the S-parameter decreases to the bulk value at the distance of about 400 μm outside the left and right edges of the impression indentation. For the load of 100 N (Fig. 2c), this distance is lower; it means about 200 μm. It can be explained that for this load, the elastic region is hidden by the large plastically deformed region. Nevertheless, a significant expansion of the defects outside the impression indentation is detected.

Feng et al. [15] considered another model called an embedded center of dilatation (ECD) model, which is a more generalized model proposed by Yoffe [16]. They took into account surface effects, which are the superposition of a Hertzian field. Unfortunately, the accuracy of our
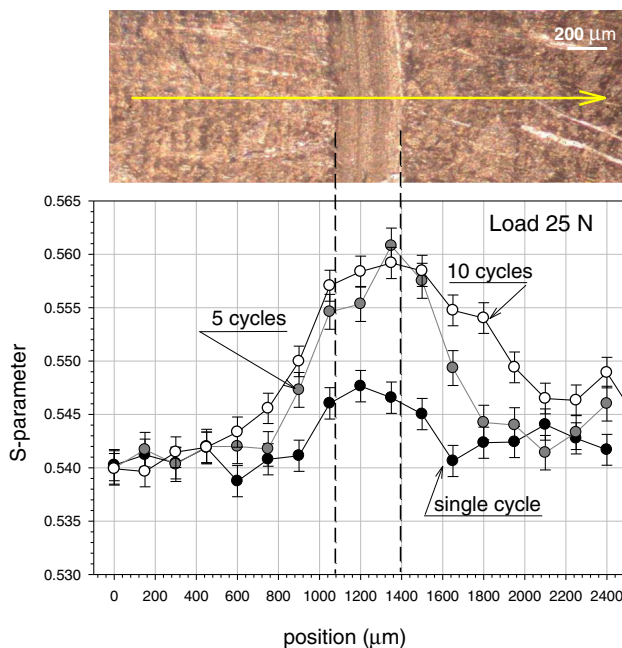
Fig. 3 The SEM picture of the wear track induced by the ball dry sliding on the surface of the well-annealed copper with the normal load of 25 N. The *arrow* indicates the direction of the positron beam scan across the track. *On the bottom*, the dependencies of the S-parameter at different points in the vicinity of the track for three different numbers of cycles, one (*black circles*), five (*gray circles*) and ten (*open circles*) cycles of the ball sliding are depicted

positron measurements is still not sufficient to test more sophisticated models of stress distribution around the indentation. Nevertheless, the future improvement of the presented experimental technique can help to test other models. More precise measurement of the annihilation line spectra, for instance, the increase of the counting time, should significantly improve the measured accuracy of the S-parameter. The reduction of the beam width is still possible and should improve the accuracy of detected dependencies.

3.2 Results for the Dry Sliding Wear Track

Our main interest was to scan the vicinity of the wear track that occurs during the dry sliding test. We argue that distribution of defects that are generated during sliding contact differs from the indentation in static conditions presented above. In this experiment, we investigated three wear tracks made when the ball slides in dry conditions on the surface of a virgin copper disc. The tracks were made in a pin-on-disc tester with the ball loaded with a normal load of 25 N. Each track was made with different numbers of cycles or turns of the disc against the ball: one cycle, five and ten cycles. At the bottom of Fig. 3, we depict the S-parameter dependency across the track made in these

conditions, and at the top of Fig. 3, the SEM picture of the track is presented. The width of the track is about 340 μm and does not depend on the number of cycles applied. It is visible that after five cycles the values of the S-parameter are saturated in the region of the track. Similarly to the results for indentation presented above, the S-parameter has the highest value in the track region, and its value decreases outside the track as well. For the sample with one cycle, the S-parameter reaches the bulk value in the distance of about 100 μm from the left edge of the track and about 400 μm from the right edge of the track. For samples with five and ten cycles, these distances are larger; for instance, for ten cycles they are about 560 μm from the left and 720 from the right edges of the track. The lack of symmetry is a characteristic feature of these results. The S-parameter in the case of the wear track reaches the bulk value at a greater distance on the right side of the track than on the left side of the track. It unambiguously indicates that defects induced by plastic and elastic deformation are expanded at a greater distance from the outer edge than inner edge of the track. The small radius of the wear track, i.e., about 7 mm, indicates the presence of a tangential force that acts outwardly from the track. We argue that the larger number of cycles will create a visible bulge in this region. Such an effect was observed by Taşan, who measured the profiles across the track; see for instance Fig. 5.3 in Ref. [17].

We performed many investigations using positron techniques of the defect depth distribution in samples below wear tracks in the interior of samples [7]. Due to the special technique, we achieved good accuracy in obtaining the total depth of the defect distribution below the worn surface, which is the total depth of the so-called subsurface zone induced by dry sliding of the ball. We established that the total depth in copper is about 300–400 μm, and this depth corresponds well with the results obtained on the surface.

4 Conclusions

The application of the positron microscopy to the studies of the defect distribution in the vicinity of ball indentation reveals the extension of the defects, induced mainly by the elastic deformation, outside the indentation. The extension region is about 200 μm on both sides of the indenter impression. A good correlation between the von Mises stress and the S-parameter distribution around the indentation is found. An asymmetric distribution of defects around the wear track induced by sliding is detected. The extension of these regions at a larger distance outside the track than inside the track results from a tangential force.

The observed range of this extension correlates with the defect depth distribution detected by other positron studies.

Appendix

Principal stresses in the rz plane are calculated using the equations [13]:

$$\sigma_{1,3} = \frac{\sigma_r + \sigma_z}{2} \pm \sqrt{\left(\frac{(\sigma_r - \sigma_z)}{2}\right)^2 + \tau_{rz}^2}, \tag{2}$$

$$\sigma_2 = \sigma_\theta, \tag{3}$$

$$\tau_{max} = \frac{1}{2}[\sigma_1 - \sigma_3]. \tag{4}$$

The above equations are obtained from the general formulae describing stresses within the interior of a sample given in cylindrical polar coordinates for a spherical indenter of radius r and a radius of the contact area a [Eq. (1)].

Radial stress distribution is given by the equation:

$$\frac{\sigma_r}{p_m} = \frac{3}{2}\left\{\frac{1-2v}{3}\frac{a^2}{r^2}\left[1-\left(\frac{z}{u^{1/2}}\right)^3\right]\right. \\ + \left(\frac{z}{u^{1/2}}\right)^3\frac{a^2u}{u^2+a^2z^2} \\ \left. + \frac{z}{u^{1/2}}\left[u\frac{1-v}{a^2+u}+(1+v)\frac{u^{1/2}}{a}\tan^{-1}\left(\frac{a}{u^{1/2}}\right)-2\right]\right\}, \tag{5}$$

where $p_m = \frac{P}{\pi a^2}$ is the mean contact pressure; P is the load; v is Poison's ratio.

The hoop stress is calculated from the equation:

$$\frac{\sigma_\theta}{p_m} = -\frac{3}{2}\left\{\frac{1-2v}{3}\frac{a^2}{r^2}\left[1-\left(\frac{z}{u^{1/2}}\right)^3\right]\right. \\ \left. + \frac{z}{u^{1/2}}\left[2v+u\frac{1-v}{a^2+u}-(1+v)\frac{u^{1/2}}{a}\tan^{-1}\left(\frac{a}{u^{1/2}}\right)\right]\right\}. \tag{6}$$

The axial stress:

$$\frac{\sigma_z}{p_m} = -\frac{3}{2}\left(\frac{z}{u^{1/2}}\right)^3\left(\frac{a^2u}{u^2+a^2z^2}\right). \tag{7}$$

The shear stress:

$$\frac{\tau_{rz}}{p_m} = -\frac{3}{2}\left(\frac{rz^2}{u^2+a^2z^2}\right)\left(\frac{a^2u^{1/2}}{a^2+u}\right), \tag{8}$$

where

$$u = \frac{1}{2}\left\{(r^2+z^2-a^2)+\left[(r^2+z^2-a^2)^2+4a^2z^2\right]^{1/2}\right\}. \tag{9}$$

Along the z axis at $r = 0$ σ_r, σ_θ and σ_z are principal stresses. The two principal stresses are equal, $\sigma_2 = \sigma_1$.

References

1. Puska, M.J., Nieminen, R.M.: Defect spectroscopy with positrons: a general calculated method. J. Phys. F: Met. Phys. **13**, 333–346 (1983)
2. Somieski, B., Krause-Rehberg, R.: Application of the positron lifetime spectroscopy as a method of non-destructive testing. Mater. Sci. Forum **175–178**, 989–992 (1995)
3. Dryzek, J., Dryzek, E.: Subsurface zone in aluminium studied by positron lifetime spectroscopy. Tribol. Lett. **17**, 147–153 (2004)
4. Coleman, P.G.: Positron Beams and Their Applications. World Scientific, Singapore (2000)
5. Fujinami, M., Jinno, S., Fukuzumi, M., Kawaguchi, T., Oguma, K., Akahane, T.: Production of a positron microprobe using a transmission remoderator. Anal. Sci. **24**, 73–79 (2008)
6. Oshima, N., Suzuki, R., Ohdaira, T., Kinomura, A., Narumi, T., Uedono, A., Fujinami, M.: Brightness enhancement method for a high-intensity positron beam produced by an accelerator. J. Appl. Phys. **103**, 094916-1-7 (2008)
7. Dryzek, J., Dryzek, E., Stegemann, T., Cleff, B.: Positron annihilation studies of subsurface zones in copper. Trib. Lett. **3**, 269–275 (1997)
8. Dryzek, J., Polak, A.: Subsurface zone studied by positron lifetime measurements. Trib. Lett. **7**, 57–60 (1999)
9. Blicharski, M., Dymek, S., Wróbel, M.: Inhomogeneities of microstructure evolved in metals under plastic deformation. J. Mat. Proc. Tech. **53**, 75–84 (1995)
10. Dryzek, J.: Charakterystyki Procesu Annihilation Pozytonów w Fazie Skondensowanej. Wydawnictwo Uniwersytetu Jagiellońskiego, Kraków (2005)
11. Dryzek, E.: Defect depth profiling after sphere indentation and blasting in aluminium and aluminium alloys detected by positron annihilation. J. Mater. Sci. **38**, 3755–3763 (2003)
12. Johnson, K.L.: Contact Mechanics. Cambridge University Press, Cambridge (1987)
13. Fischer-Cripps, A.C.: Introduction to Contact Mechanics. Springer, New York (2000)
14. Hertz, H.: On hardness. Verh. Ver. Beförderung Gewerbe Fleisses **61**, 410 (1882). Translated and reprinted in English in "Hertz's Miscellaneous Paper", Macmillan & Co, London (1896)
15. Feng, G., Qu, S., Huang, Y., Nix, W.D.: An analytical expression for the stress field around an elastoplastic indentation/contact. Acta Mater. **55**, 2929–2938 (2007)
16. Yoffe, E.H.: Elastic stress-field casued by indentating brittle materials. Philos. Mag. A-Phys. Condens. Matter. Struct. Defects Mech. Prop. **46**, 617 (1982)
17. Taşan, Y C.: Measurement of Deformation in Rolling and Sliding Contacts. Ph.D. Thesis, University of Twente, Enschede, The Netherlands (2005)
18. Schaefer, H.-E.: Investigation of thermal equilibrium vacancies in metals by positron annihilation. Phys. Stat. Sol. (a) **102**, 47 (1987)